Mapping Built-up Areas from Multitemporal Interferometric SAR Images – A Segment-based Approach

Leena Matikainen, Juha Hyyppä, and Marcus E. Engdahl

Abstract

Automatic mapping of built-up areas from a multitemporal interferometric ERS-1/2 Tandem dataset was studied. The image data were segmented into homogeneous regions, and the regions were classified as built-up areas, forests, and open areas using their mean intensity and coherence values and additional contextual information. Compared with a set of reference points, an overall classification accuracy of 97 percent was achieved. The classification process was highly automatic and resulted in homogeneous regions resembling a map drawn by a human interpreter. The feasibility of the imagery for dividing built-up areas further into subclasses was also investigated. The results suggest that low-rise areas, high-rise areas, and industrial areas are difficult to distinguish from each other. On the other hand, a correlation between the building density, the proportion of land covered with buildings, and intensity/coherence in the image data was found. The dataset thus appeared to be promising for classifying built-up areas into subclasses according to building density.

Introduction

The development of methods for automated mapping and map updating using remotely sensed data is currently an important topic for research. In addition to aerial photographs and optical satellite imagery, synthetic aperture radar (SAR) data attract increasing attention (see e.g., Henderson and Xia, 1997; Tupin *et al.*, 1999; Borghys *et al.*, 2002; Dierking and Skriver, 2002; Haack *et al.*, 2002; Bentabet *et al.*, 2003; Dekker, 2003; Grey and Luckman, 2003; Grey *et al.*, 2003; Quartulli and Datcu, 2003). SAR images provide information complementary to that obtained from optical data (Hellwich *et al.*, 2001) and can be useful even if acquisition of optical images is difficult due to cloudiness or darkness. In the future, the importance of SAR data in mapping applications is expected to increase thanks to new systems providing data with high spatial resolution (e.g., COSMO-SkyMed) and with a variety of frequencies (e.g., TERRASAR), polarization modes and incidence angles (e.g., RADARSAT-2).

Previous studies have shown that inter+ferometric SAR data including coherence information, as well as conventional backscatter intensity, offer considerable potential for land-use mapping (Askne and Hagberg, 1993; Wegmüller and Werner, 1995 and 1997; Dammert *et al.*, 1999; Strozzi *et al.*, 2000; Weydahl, 2001; Engdahl and Hyyppä, 2003). Coherence is the correlation between the complex images of an interferometric image pair and provides information on the stability of the target (see e.g., Wegmüller and Werner, 1995). For example, forests have typically lower coherence values than open or urban areas, and interferometric SAR data are thus well suited for distinguishing forest from other land-cover classes (Wegmüller and Werner, 1995 and 1997; Smith and Askne, 2001). Since the level of coherence is related to the amount of vegetation, coherence information is also promising for quantitative forest and crop monitoring applications (see e.g., Engdahl *et al.*, 2001; Fransson *et al.*, 2001; Blaes and Defourny, 2003; Pulliainen *et al.*, 2003). Extraction of linear objects from interferometric SAR data in the Siberian lowlands and in a rain forest context has been studied by Hellwich *et al.* (2002) and Onana *et al.* (2003), respectively.

In urban areas, the coherence is usually high due to the stability of scatterers and remains high even over long time periods (Strozzi and Wegmüller, 1998; Usai and Klees, 1999; Grey and Luckman, 2003). The coherence information is thus also valuable in urban mapping. In backscatter intensity data, built-up areas are characterized by strong reflections from man-made objects such as buildings (see e.g., Dong *et al.*, 1997). The heterogeneous appearance of the areas in the imagery, however, can make automatic interpretation difficult. For example, a suburban area typically comprises houses, roads, other construction, yards, and different types of vegetation. In an image with a spatial resolution of about 30 m, this area appears as a group of mixed pixels together with pure pixels from various land-cover classes. As discussed by Xia and Henderson (1997), the factors affecting the intensity of radar returns from surface objects, especially for urban environments, are many, varied, and complex.

Several studies related to urban mapping from interferometric SAR data have been conducted. Strozzi and Wegmüller (1998), Del Frate *et al.* (1999), and Santoro *et al.* (1999 and 2000) tested different approaches based on coherence, intensity and texture information to detect urban areas. Del Frate *et al.* (1999) and Santoro *et al.* (1999) also discussed the possibility of classifying urban areas into subclasses, such as areas with different building densities. Grey and Luckman (2003) used coherence information to map urban extent, and Grey *et al.* (2003) applied coherence information in mapping urban

Leena Matikainen and Juha Hyyppä are with the Finnish Geodetic Institute, Department of Remote Sensing and Photogrammetry, P.O. Box 15, FI-02431 Masala, Finland (Leena.Matikainen@fgi.fi; Juha.Hyyppa@fgi.fi).

Marcus Engdahl is currently with ESA/ESRIN, Via Galileo Galilei, Frascati, Italy, and formerly with Helsinki University of Technology, Laboratory of Space Technology, Finland (Marcus.Engdahl@esa.int).

Photogrammetric Engineering & Remote Sensing
Vol. 72, No. 6, June 2006, pp. 701–714.

0099-1112/06/7206–0701/$3.00/0

change. Grey and Luckman (2003) found that classification kappa coefficients greater than 90 percent can be achieved in urban/non-urban classification when image pairs with long time intervals between the images are used. Fanelli *et al.* (2000) analyzed the causes of decorrelation in urban areas, and Fanelli *et al.* (2001) and Luckman and Grey (2003) studied the use of coherence images to acquire information on building heights. The mapping of urban areas has also been addressed in land-cover mapping studies with a larger number of classes (Wegmüller and Werner, 1997; Dammert *et al.*, 1999; Strozzi *et al.*, 2000). For example, Strozzi *et al.* (2000) used different algorithms and test areas in Europe and their results suggested that land-use classification accuracies of around 75 percent are possible with, in the best case, simultaneous forest and non-forest accuracies of around 80 to 85 percent. The accuracy of urban areas, however, was only around 30 percent. Problems in discriminating urban areas were also encountered by Dammert *et al.* (1999). In these previous studies, various numbers of European Remote Sensing Satellite (ERS) SAR images and features extracted from them have been used. The classification algorithms applied were pixel-based methods.

The goal of our study was to investigate how built-up areas could be detected automatically from a multitemporal interferometric ERS-1/2 Tandem dataset using a region-based classification approach and to evaluate the applicability of the data to automatic land-use mapping and map updating. Previous studies have shown that the classification results of remotely-sensed data can be improved by using spatial information, for example segmenting the image into homogeneous regions before classification (see e.g., Kettig and Landgrebe, 1976; Johnsson, 1994; Dong *et al.*, 2001; Borghys *et al.*, 2002; Macrì Pellizzeri *et al.*, 2003). Classification of regions is easier than classification of single pixels, especially in heterogeneous images. In addition, a region-based approach allows advanced use of contextual information such as neighborhood relationships in classification (see Benz *et al.*, 2004). Previous studies have also shown that use of spatial information in the form of textural features is advantageous for classification (see e.g., Ulaby *et al.*, 1986; Schistad Solberg and Jain, 1997; Karathanassi *et al.*, 2000; Rajesh *et al.*, 2001; Shaban and Dikshit, 2001; Gluch, 2002; Haack *et al.*, 2002; Kiema, 2002; Dekker, 2003; Dell'Acqua and Gamba, 2003). Many of these studies have concentrated on urban areas where a heterogeneous landscape makes pixel-based classification of the original image data especially difficult.

A dataset created from 14 ERS-1/2 complex image pairs acquired during the ERS Tandem mission in 1995–1996 (Engdahl and Hyyppä, 2003) was used in the study. The imagery covers Helsinki and its surroundings with a variety of built-up areas as well as forests and agricultural land. According to visual evaluation, the dataset is promising for land-use mapping applications. Forests, agricultural fields, urban areas, and even main roads and railways are visible in the imagery. Due to the relatively low spatial resolution of the ERS data, automatic extraction of small or narrow objects, such as roads, is likely to be difficult and was not investigated in the study, but for mapping land-use classes in a coarser scale the dataset could be useful. Engdahl and Hyyppä (2003) achieved an overall accuracy of 90 percent when classifying the dataset into six classes using a pixel-based approach. They used a thresholding rule based on two Tandem pairs to detect water and an unsupervised ISODATA classifier to classify the other classes.

Study Area and Data

Study Area

The study area covers Helsinki and its surroundings in southern Finland. This area comprises a variety of built-up areas, forests, and agricultural land. The total land area covered with the imagery and classified in the study is about 1800 km^2. For analysis and accuracy estimation, two 9.5 $\times$ 9.5 km sub-areas were used. They will be referred to as Test Site 1 and Test Site 2. The test sites are mainly suburban areas located about 5 to 20 km west of the center of Helsinki. In addition to the test sites, a few training areas were used in land-use classification and a set of reference points in accuracy estimation. A figure of the study area showing the location of the test sites, training areas and reference points is shown in Figure 1. Use of the different subareas and reference data sources in the study is summarized in Table 1.

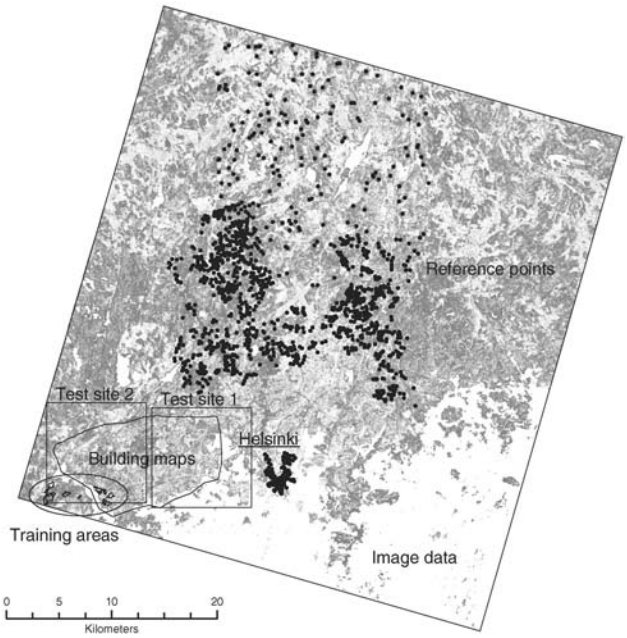

Figure 1. Study area around Helsinki in southern Finland. Channel 2 of the image dataset is shown in the background, water mask is shown in white. Image data obtained from ESA AO3-277.

TABLE 1. USE OF DIFFERENT SUBAREAS AND REFERENCE DATA SOURCES IN THE STUDY

	Land-use Classification		Building Density Classification	
	Training	Accuracy Estimation	Training	Accuracy Estimation
Training areas	X			
Reference points		X		
Test Site 1				
a) Reference data based on the 1:50 000 Map Database and a forest map		X	(X)	
b) Building maps (cover part of Test Site 1)			X	
Test Site 2				
Building maps (cover part of Test Site 2)				X

SAR Imagery

A total of 14 ERS-1/2 Tandem complex image pairs acquired in 1995 and 1996 from descending orbits were processed using a commercial software package from GAMMA Remote Sensing Research and Consulting AG (GAMMA Remote Sensing, 2004). Processing the data was described in detail in Engdahl and Hyyppä (2003), and 28 intensity, 14 coherence, and 2 long-time coherence (with temporal baselines of 36 and 246 days) images were created and orthorectified. The pixel size of the images after processing was 20 × 20 m. The intensity and coherence images were filtered separately with a temporal filter. To acquire the spatial estimates needed in temporal filtering, a 5 × 5 pixel k-nearest-neighbor Lee and a 5 × 5 pixel median filter were used for the intensity and coherence images, respectively. The principal components transformation (PCT) was used to reduce the dimensions of the dataset. A textural feature, grey-level co-occurrence matrix (GLCM) uniformity (ER Mapper, 2002), was calculated from the intensity images. This feature was first calculated separately for each of the 14 Tandem mean intensity images using a 9 × 9 pixel window, and the results were then averaged. The applied direction of co-occurrence was 135 degrees (clockwise from north). A water mask was created by thresholding backscatter intensity ratio images (Engdahl and Hyyppä, 2003). The final image dataset applied in the present study included eight channels with values scaled into range 0 to 255:

1. Temporal average of the backscatter intensity images,
2. Temporal average of the Tandem coherence images,
3. Average of two coherence images with long temporal baselines,
4. The 1st principal component (PC) calculated from the Tandem coherence images,
5. The 2nd PC calculated from the Tandem coherence images,
6. The 1st PC calculated from the backscatter intensity images,
7. The 2nd PC calculated from the backscatter intensity images, and
8. Textural feature calculated from the backscatter intensity images (GLCM uniformity)

Water areas were excluded from the study by using the water mask as a thematic layer in segmentation and classification.

Reference Data for Estimating the Accuracy of Land-use Classification

A set of 1,313 reference points determined and described by Engdahl and Hyyppä (2003) was used as reference data in estimating the accuracy of land-use classification results. Aerial photographs, topographic maps and information from the National Forest Inventory of Finland were used to determine the reference points that represent seven land-cover classes: open area, sparse forest, dense forest, low-rise residential area, high-rise residential area, dense urban area (city center), and industrial area.

In addition to the reference points, a reference map based on two digital map datasets and covering Test Site 1 was used in accuracy estimation (see Plate 1). Low-rise areas (areas of small houses), high-rise areas, industrial areas, fields, meadows, and open areas were obtained from the 1:50 000 Map Database of the National Land Survey of Finland (NLSF), and forests were obtained from a forest map of FM-Kartta Oy. The map data for the three built-up and three open classes were converted from vector into raster format with 20 × 20 m pixels. Created from aerial images, the forest map was originally very detailed and was first converted into a raster map with 2 × 2 m pixels. The reference map with the built-up and open areas was then

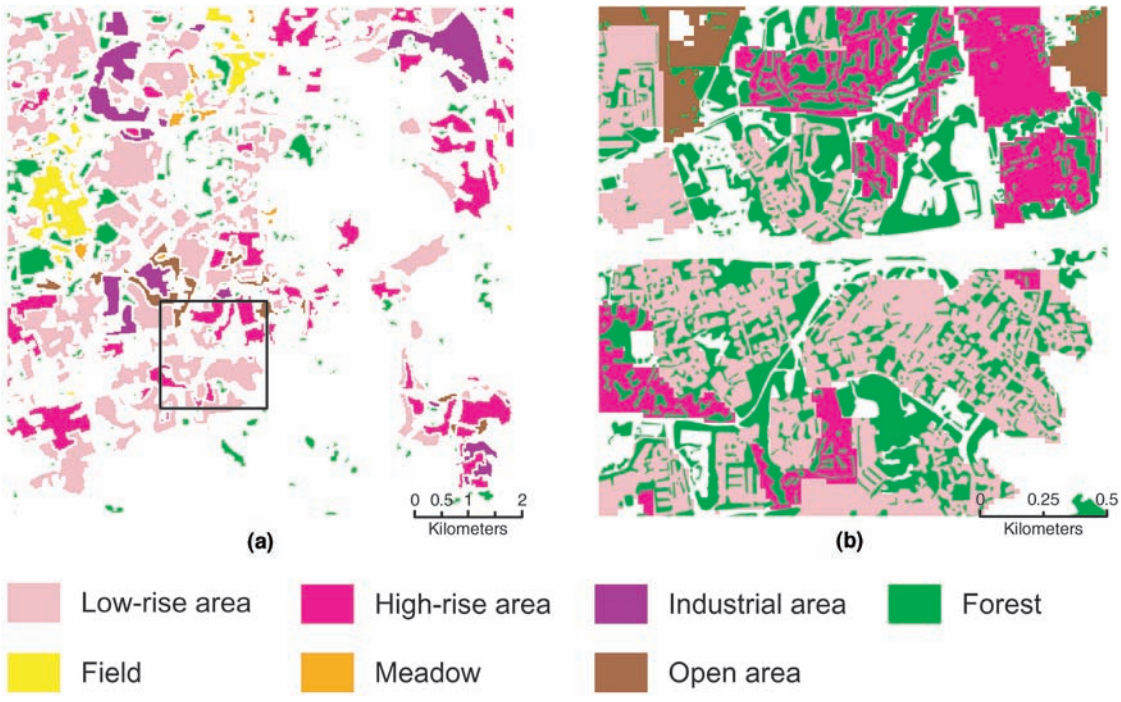

Plate 1. (a) Reference map for estimating the accuracy of land-use classification in Test Site 1 (based on the 1:50 000 Map Database and a forest map). The map is in raster format with 20 × 20 m pixels, and the boundary pixels of classes have been excluded; (b) Original map data for the subarea marked with a square on Plate (a) (1:50 000 Map Database data converted into raster format and forest polygons from the forest map). (1:50 000 Map Database data © The National Land Survey of Finland, permission number 827/MYY/04. Forest map © 2002, FM-Kartta Oy)

supplemented with the forest data; if a pixel was unclassified in the reference map and completely covered with forest in the forest map, it was labeled as forest. Finally, all boundary pixels of classes were labeled as unclassified to exclude possibly uncertain and mixed pixels from the accuracy estimation.

It should be noted that the reference map provides information on the occurrence of seven land-use classes in the area, but it does not cover the area exhaustively. For example, large individual buildings are typically presented as buildings in the 1:50 000 map and areas with this type of buildings are not included in the built-up areas. Similarly, open areas other than those classified as fields, meadows and open areas also occur in the area. Those three classes were selected because they should represent clearly open areas without ambiguities. The 1:50 000 Map Database in Test Site 1 corresponded to the situation in 1996 and was thus well-suited for analysis of the imagery from 1995 and 1996. The forest map was for 2001. Areas covered with forest in the map were most likely also covered with forest in 1995 and 1996, but if some forest was felled after 1995 and 1996, it is missing in the reference map. Many forests are also missing in the reference map due to the very detailed representation in the original map (pixels can be included in built-up areas or labeled as unclassified, see Plate 1).

Reference Maps for Analyzing Built-up Areas

Built-up areas of the 1:50 000 Map Database in Test Site 1 were used in analyzing the appearance of different types of built-up areas (low-rise areas, high-rise areas, and industrial areas) in the imagery. A raster map with 20 $\times$ 20 m pixels was created as described above. In this case, only built-up areas were included in the map and boundary pixels were not excluded.

To study the relationship between values in the imagery and building density, two building maps in raster format were created. The pixel size of the maps is 2 $\times$ 2 m, and the maps cover most of Test Site 1 (see Figure 1). Both maps are based on the Topographic Database of the NLSF, and a building map and a digital elevation model (DEM) of FM-Kartta Oy. One of the maps corresponds to the situation in 2000, which was presented in the Topographic Database. The other is based on an edited version of the database and approximately represents the situation in 1995 and 1996. In the following, the reference maps will be referred to as the *new building map* and the *old building map*, respectively.

Outlines of the buildings in the reference maps were taken from the Topographic Database, and building heights are based on the building map and DEM obtained from FM-Kartta Oy. Each building pixel in the reference maps has the height of the building as its value. It must be noted that due to matching problems with the two original vector maps (the Topographic database and the building map of FM-Kartta Oy), some errors in building heights occur in the reference maps, especially in buildings with complex shapes. About 8 percent of buildings had a height value of 0 m, and for these buildings the mean height of buildings of the same class (classes defined in the Topographic Database) in Test Site 1 was assigned. For most buildings, however, the height information is correct. Since the building maps were used in analyzing regions, not individual buildings, it can be expected that the errors did not have a remarkable effect on the results.

Reference Maps for Estimating the Accuracy of Building Density Classification

Building maps from Test Site 2 (see Figure 1) were used in estimating the accuracy of a building density classification carried out in the study. An *old building map* and a *new building map* were created in a similar way as in Test Site 1 (see above). The new building map corresponds to the situation in 2000 and is thus a few years newer than the imagery. On the other hand, the old building map in Test Site 2 represents the situation a few years before the images were acquired.

Methods

General

In the first stage of the study, the objective was to distinguish built-up areas from other land-use classes, and classification of the image data into main land-use classes was thus performed. The class *built-up area* was defined to include buildings, roads, and other man-made structures of an urban environment, as well as small vegetation-covered areas related to them, such as gardens. The feasibility of the imagery for classifying built-up areas further into subclasses was then investigated, and a building density classification was conducted. The accuracy of the classification results was estimated by comparing them with reference data. The overall flow of the study is presented in Figure 2. A region-based approach was used throughout the study; the imagery was segmented into homogeneous regions before classification, and all analyses were performed for regions (i.e., segments). eCognition software (Definiens Imaging, 2004) was used in segmentation and classification. Statistical analysis of built-up areas and accuracy estimation were conducted using MATLAB (The MathWorks, 2004).

The applied multi-resolution segmentation method (Baatz and Schäpe, 2000; Definiens Imaging, 2003) is based on bottom-up region merging and a local optimization process minimizing the growth of a given heterogeneity criterion. The heterogeneity criterion is defined as a combination of spectral (color) and spatial heterogeneity. The spectral heterogeneity of segments is based on the sum of the standard deviations of spectral values in different channels (digital numbers in the SAR data in our study), weighted with channel weights, while the spatial heterogeneity is based on the compactness and/or smoothness of the segments. The compactness of a segment is measured by calculating the ratio of its border length to the square root of its area. The smoothness is measured by the ratio of the border length to the shortest

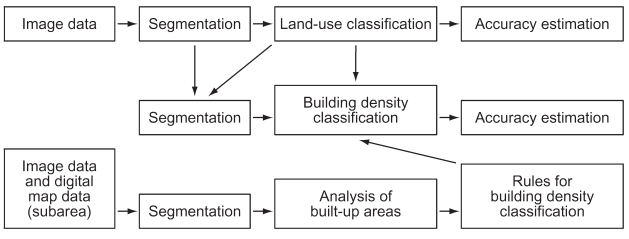

Figure 2. Flow of the study. The image data were first segmented and classified into land-use classes (top of the figure). The feasibility of the imagery for classifying built-up areas further into subclasses was then investigated using a subarea of the data (bottom), and rules defined from this analysis were used to classify built-up areas of the land-use classification result into building density classes (middle). The accuracy of the classification results was estimated by comparing them with reference data.

possible border length, which is determined on the basis of the bounding box of the segment. The heterogeneity measures are weighted by segment sizes. The size and number of resulting segments is controlled with a scale parameter, which is a measure for the maximum change in heterogeneity that may occur when two segments are merged. The segmentation method allows creation of several hierarchical levels of segments with different sizes. These levels form an image object hierarchy, in which a segment on a higher level can consist of several subsegments on a lower level. It is also possible to use map information as thematic layers to guide the segmentation so that each segment belongs to only one class of the map. A classification-based segmentation can be produced after preliminary segmentation and classification steps.

In classification, the nearest neighbor (NN) classification method and membership functions were used (Definiens Imaging, 2003). The NN method is a flexible classification method because it does not require the data to have a certain statistical distribution. For each segment, the most similar sample object (segment) is found and the segment is assigned to the same class with this sample object as described in Definiens Imaging (2003). Similarity is measured by calculating distances in the feature space (Euclidean distances calculated using feature values that are divided by the standard deviation of all values for the feature). By using membership functions, on the other hand, it is possible to define various rules for classification. For example, neighborhood relationships between segments can be exploited.

Land-use Classification

The image data were first segmented into relatively small and homogeneous regions using channels 1 through 3 with equal weights, a scale parameter of 15, and a heterogeneity criterion: color 80 percent, shape 20 percent (smoothness 90 percent, compactness 10 percent). Appropriate parameter values were found heuristically (which also applies to other stages of the study). The effect of given parameter values is dependent on the image data used, and the values are thus not generally applicable. They are reported here to give a rough idea of similarities and differences between segmentation results used in various stages of the study. The heterogeneity criterion corresponded to the default values of the software. The mean area of the resulting segments was about 2 ha. Segments in built-up areas were often smaller than segments in forested and open areas.

Training areas for recognizing built-up areas, forests, and open areas with the NN classifier were defined manually on the basis of the image data, maps and knowledge of the region. The initial training areas covered 0.12 percent of the total land area in the imagery and included four built-up areas in a suburban area containing both a densely built-up area and a low-rise residential area, two forest areas, two open areas on agricultural fields, and one on a golf course. The training areas for the built-up class covered mixed pixels of buildings and other land-covers in addition to a pure densely built-up area. The initial training areas were imported into eCognition as a training area mask, and sample objects were automatically created. Finally, the sample objects were checked manually using digital map data. Some corrections were made. The training areas did not have any overlap with the reference data used in estimating the accuracy of land-use classification.

The NN classification method was used to classify the segments into built-up areas, forests and open areas using the mean values of the segments in various image channels.

The following channel combinations were used:

- Channels 1 through 3, which are well-suited to visual interpretation (see Plate 2a).
- Channels 2 through 6 with and without texture channel 8; these were the most useful channels according to preliminary analysis of training area statistics.
- Channels 1 through 8, i.e., all channels.

Complete detection of built-up areas, especially low-rise areas, can be difficult if only the mean intensity and coherence values of the segments are used in classification. In low-rise areas a major part of the land is covered with vegetation and contextual information on the neighborhood is needed to include these vegetated areas into the built-up land-use class. The texture channel of the dataset was created to provide this type of contextual information. As another alternative, use of information on the classes of neighboring segments was tested. In practice, a new segmentation level identical to the first level was created to allow another classification to be performed for the same segments. The new segments were first classified according to the previous result, and forests and open areas were then further divided into urban forest, other forest, urban open, and other open using neighborhood relationships (Definiens Imaging, 2003). A segment became classified as urban forest or urban open if over 50 percent of its border was surrounded by built-up area. Urban forest and urban open were then grouped together with the built-up area. Finally, the classification results were compared with the reference data to estimate the accuracy of land-use classification.

Analysis of Built-up Areas: Comparison of Low-rise Areas, High-rise Areas, and Industrial Areas

The feasibility of distinguishing low-rise areas, high-rise areas, and industrial areas from each other from the imagery was studied using 1:50 000 map data from Test Site 1. Histograms of various segment attributes in the three classes were compared. Segmentation was performed using image channels 1 through 3. Small segments corresponding to those used in land-use classification were first created. Segmentation was then continued with a scale parameter of 40 and a heterogeneity criterion: color 50 percent, shape 50 percent (smoothness 50 percent, compactness 50 percent). The purpose was to create larger regions that might be useful for representing different types of built-up areas in a map. The map showing the three classes of built-up areas was used as a thematic layer in segmentation. Each segment thus belonged completely to one class in the map, which made it possible to compare the properties of segments from different classes. The mean area of the built-up segments was about 8 ha. The final segmentation result together with various attributes of the segments (mean values and standard deviations in each channel, textural features) was exported from eCognition, and histograms of the attribute values were formed for the three classes.

Analysis of Built-up Areas: Relationship Between Image Data and Building Density

The relationship between the mean values of segments in the imagery and building density was studied using building maps from Test Site 1. Segmentation was performed without map data, but otherwise with similar parameters as described in the previous section. A mask showing the coverage of the building maps (see Figure 1) was used as a thematic layer to obtain segments that were completely covered with the maps. The mean area of the

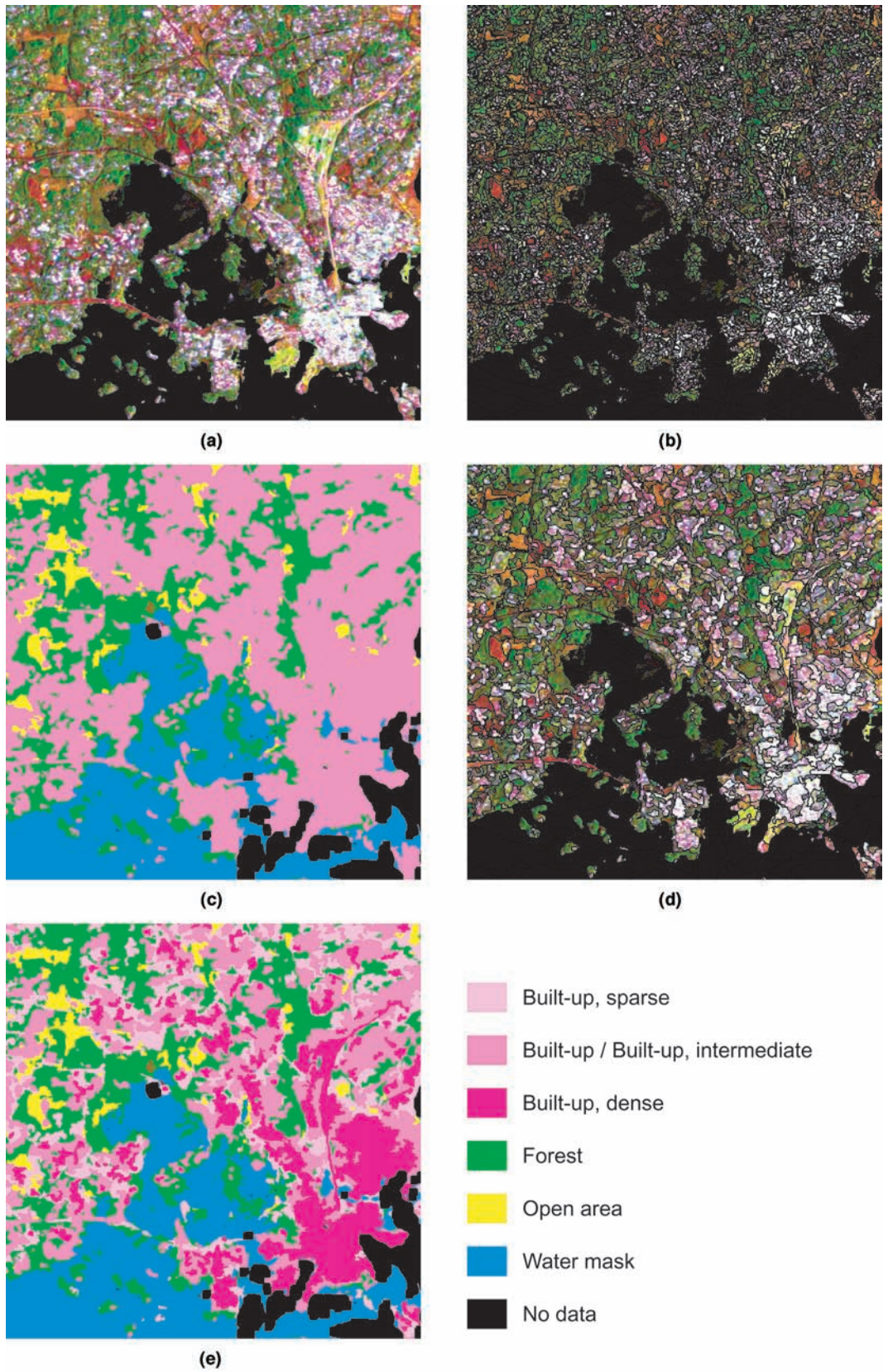

Plate 2. (a) A 12 × 12 km subarea of the imagery (Red: channel 2, Green: channel 1, Blue: channel 3). (b) Segments for land-use classification. (c) Land-use classification result based on channels 2 through 6 and 8. (d) Segments for building density classification. (e) Result of building density classification. Image data obtained from ESA AO3-277.

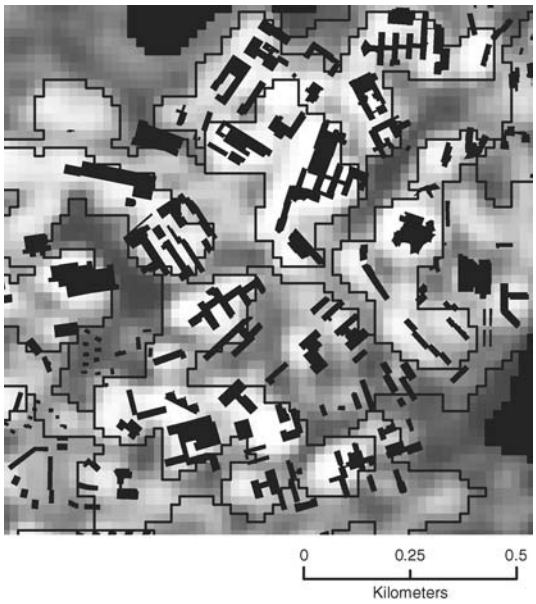

Figure 3. Building polygons overlaid on the segmentation result. The building map was used in calculating the building density of the segments. Image data obtained from ESA AO3-277. (Buildings © The National Land Survey of Finland, permission number 827/MYY/04)

segments was about 17 ha (both built-up and other segments included). The results were exported from eCognition, and for each segment, two building density measures were calculated from the building maps (see Figure 3). The first one was calculated by dividing the area covered with buildings by the total area of the segment. In the other measure, building heights were taken into account by dividing the total building volume of the segment by the area of the segment. Scatter plots showing the relationship between the mean values of segments in different channels and building density were then formed. Linear regression and histogram analyses were also conducted.

Building Density Classification

On the basis of threshold values determined from the analysis, all built-up areas detected in the land-use classification stage (the best classification result compared with reference data) were further classified into three building density classes in eCognition. This classification was applied for segments created with a scale parameter of 40 and a heterogeneity criterion: color 50 percent, shape 50 percent (smoothness 50 percent, compactness 50 percent) (the same parameter values that were used in the analysis stage). The segmentation level was created between the original small segments used in land-use classification and large segments determined from the land-use classification result. Each new segment thus belonged completely to one land-use class, which made classification of built-up segments into subclasses possible. As before, channels 1 through 3 were used in segmentation. The mean area of the resulting built-up segments was about 8 ha. Finally, the classification results were compared with reference data (building densities calculated from the building maps of Test Site 2) to evaluate the accuracy.

Results and Discussion

Land-use Classification

The accuracy of the land-use classification results compared with the reference points and the reference map is presented in Table 2. The table shows the percentage of correctly classified reference data (corresponds to interpretation accuracy or producer's accuracy and total accuracy or overall accuracy) using various combinations of the channels. The segmentation result for part of the study area is presented in Plate 2b and the classification result obtained using channels 2 through 6 and 8 is presented in Plate 2c. Confusion matrix and accuracy estimates for this classification are shown in Table 3 (for description of the accuracy measures, see Helldén, 1980). To create the confusion matrix, the reference points were used and combined into three classes corresponding to those used in the classification: open area, forest (contains points of sparse and dense forest), and built-up area (contains points of low-rise residential area, high-rise residential area, dense urban area, and industrial area).

As shown by the results in Table 2, a high accuracy was achieved in the land-use classification. Compared with the reference points, all the channel combinations tested gave an overall classification accuracy better than 90 percent. The best result (97 percent) was obtained using channels 2 through 6 and 8 (channels containing coherence information,

TABLE 2. ACCURACY OF LAND-USE CLASSIFICATION RESULTS COMPARED WITH THE REFERENCE POINTS AND REFERENCE MAP

Type of Reference Data Class (number of pixels)	Correct Classification Result	% of Pixels in Reference Class Correctly Classified					
		Channels used					
Reference Points		1–3	1–3*	2–6	2–6*	2–6,8	1–8
Open area (583)	Open	96	92	98	96	97	94
Sparse forest (77)	Forest	91	91	96	96	94	96
Dense forest (112)	Forest	98	98	98	98	98	99
Low-rise residential area (156)	Built-up	66	79	67	74	94	93
High-rise residential area (198)	Built-up	87	97	93	98	96	96
Dense urban area (city center) (92)	Built-up	100	100	100	100	100	100
Industrial area (95)	Built-up	93	94	97	98	99	99
All classes (1313)		91	92	94	94	97	96
Reference Map							
Field (3598)	Open	77	77	92	89	93	91
Meadow (501)	Open	47	46	44	40	54	54
Open area (1442)	Open	65	51	44	30	38	32
Forest (5520)	Forest	96	91	97	94	93	94
Low-rise area (24841)	Built-up	61	77	62	75	78	77
High-rise area (11805)	Built-up	89	98	91	97	96	97
Industrial area (6325)	Built-up	89	96	94	97	99	99
All classes (54032)		75	84	77	84	86	85

*Accuracy after the second classification step using neighborhood information.

TABLE 3. CONFUSION MATRIX AND ACCURACY ESTIMATES FOR THE LAND-USE CLASSIFICATION RESULT BASED ON CHANNELS 2 THROUGH 6 AND 8. REFERENCE POINTS WERE USED AS REFERENCE DATA

	Reference Class			
Classification Result	Open	Forest	Built-up	Sum
Open	567	5	3	575
Forest	3	182	14	199
Built-up	12	2	524	538
Unclassified	1	0	0	1
Sum	583	189	541	1313
Interpretation accuracy	97%	96%	97%	
Object accuracy	99%	91%	97%	
Mean accuracy	98%	94%	97%	
Overall accuracy				97%

the first PC calculated from the intensity images, and texture). Table 3 shows that the accuracy of this classification result was high for each of the three classes; the mean accuracies for built-up area, forest, and open area were 97 percent, 94 percent, and 98 percent, respectively. Using all channels, nearly the same overall accuracy was achieved (96 percent, Table 2). Compared with the reference map, the accuracy was generally somewhat lower than compared with the reference points. The overall accuracy of the best classification result was 86 percent.

Reference points in dense urban areas (city center) were recognized as built-up with 100 percent accuracy in each classification (Table 2). In low-rise residential areas, high-rise residential areas, and industrial areas, the percentage of reference points correctly classified as built-up was 66 to 94 percent, 87 to 98 percent, and 93 to 99 percent, respectively. The texture channel 8 appeared to be useful in recognizing built-up areas, especially low-rise areas, as built-up. It is worth noting that the mean value of the textural feature for each segment was used in classification, but due to the pixel-based calculation of the texture channel with a relatively large window size of 9×9 pixels, the mean value for a given segment was based on intensity variations both in the segment and its neighborhood. The texture channel thus brought some contextual information into classification. When the texture channel was not used, the interpretation accuracy of built-up areas could be clearly improved by using information on the classes of neighboring segments. For example, when using channels 1 through 3, the second classification step with the neighborhood information improved the percentage of low-rise residential areas and high-rise residential areas recognized as built-up from 66 percent to 79 percent and from 87 percent to 97 percent, respectively, compared with the reference points. On the other hand, this classification step decreased the percentage of correctly classified open areas and forests; that is, some open areas and forests were incorrectly classified as built-up. In high-rise areas and industrial areas, the accuracy compared with the reference map was nearly the same as the accuracy compared with the reference points. In low-rise areas, the accuracy of the best classification results (channel combinations 2 through 6 and 8, and 1 through 8) was clearly lower when compared with the reference map. With the channel combination 2 through 6 and 8, 78 percent of the low-rise areas in the reference map were classified as built-up. The corresponding result calculated using the reference points was 94 percent. Visual comparison of the results with the map and image data revealed that the low-rise areas which were not detected were often forested areas and not clearly visible in the imagery. On the other hand, small areas in forest, especially rocky or hilly areas, were sometimes misclassified as built-up.

It should be noted that the two reference data sources (points and map) differed much from each other. The points are distributed over a large part of the study area and represent homogeneous plots selected manually using e.g., aerial imagery (Engdahl and Hyyppä, 2003). The map, on the other hand, provides more complete coverage for a relatively small area but contains information that has been generalized for map presentation. In the reference map, the relative proportion of built-up land is clearly larger than in the reference points and in the study area in general, which also affected the results. The lowest accuracy was obtained for the meadows and open areas of the reference map. The number of meadows and open areas in Test Site 1 was small, and it is thus difficult to draw any conclusions on the results. In the case of meadows, some confusion occurred with forests, but the meadows were small in size. In the case of open areas, the most confusion occurred with built-up areas. This is probably related to the relatively small size of the open areas compared with the spatial resolution of the imagery and definition of the classes. Use of contextual information in classification helped to include small, vegetated areas in the urban environment into the built-up land-use class. This was advantageous for mapping low-rise areas as built-up, but on the other hand decreased the accuracy of open areas, which can be seen in Table 2.

The classification results, especially for built-up areas, were clearly better than those obtained in some previous studies with interferometric ERS data (e.g., Strozzi *et al.*, 2000), although it must be noted that direct comparison of classifications with different datasets, class definitions, and number of classes is impossible. The main explanation for the good accuracy achieved in the present study is probably the high quality of the interferometric dataset. Engdahl and Hyyppä (2003) achieved an overall accuracy of 90 percent when applying an unsupervised pixel-based ISODATA classification to the same dataset (channels 1 through 6 used in classification, the reference points in accuracy estimation). The output from the ISODATA algorithm was filtered with a 3×3 pixels majority filter. In their final results, six classes were included (one of these was water that was detected before the unsupervised classification using a thresholding rule). Two built-up classes, mixed urban and dense urban, were included, and the interpretation accuracies (producer's accuracies) for these were 80 percent and 91 percent, respectively (mixed urban included low-rise residential areas, high-rise residential areas, and industrial areas). If the two classes were combined in the final result, the accuracy of built-up would approach the best accuracy obtained in the present study (Engdahl and Hyyppä: 92 percent of mixed urban and 100 percent of dense urban reference points classified as built-up). The accuracy of open areas and forests was nearly the same as in the present study (Engdahl and Hyyppä: 97 percent of open points classified as open, 94 percent of sparse forest, and 99 percent of dense forest points classified as forest). It can be concluded, however, that the region-based approach applied in the present study has some benefits compared with pixel-based classification. Reliable classification results are easier to achieve for segments than for single pixels because the mean values of the segments can be used. In addition, contextual information on the classes of neighboring segments can be exploited. A region-based classification also results in homogeneous regions, resembling a map drawn by a human interpreter, without any postprocessing. It is also worth noting that the classification of the present study was highly automatic; training areas covered only

about 0.12 percent of the study area and did not have any overlap with the reference data used in accuracy estimation. A disadvantage of region-based classification is that classification errors affect entire segments.

Analysis of Built-up Areas: Comparison of Low-rise Areas, High-rise Areas, and Industrial Areas

The feasibility of distinguishing low-rise areas, high-rise areas, and industrial areas from each other from the imagery was studied using data from Test Site 1 as described in the methods section. Histograms of the three classes are shown for each image channel in Figure 4. The histograms were calculated from the mean values of the segments.

As Figure 4 shows, low-rise areas, high-rise areas and industrial areas appeared to be difficult to distinguish from each other. Despite some characteristic features (e.g., low coherence values and high textural feature values in low-rise areas), a remarkable overlap exists between the histograms of different classes. Better results were not obtained when standard deviations and some textural features calculated for segments (GLCM homogeneity, GLCM contrast, and grey-level difference vector (GLDV) angular 2nd moment) (Definiens Imaging, 2003) were investigated. The results are not surprising, because areas with varying building density and vegetation cover can occur in each of the three classes.

Analysis of Built-up Areas: Relationship Between Image Data and Building Density

The relationship between the mean values of segments in the imagery and building density was studied using building maps from Test Site 1. Scatter plots showing the relationship in different channels are shown in Figure 5. The building densities in the figure were calculated from the old building map. To ensure that the building densities corresponded well to the situation at the time of image acquisition, only those segments were included for which the difference in building density calculated from the old and new maps was under 0.01 (calculated without building heights). The brightness of a segment in Figure 5 was calculated in eCognition as the mean value of the mean values of the segment in image channels 1 through 5.

Linear regression analyses between the mean values of segments and the building density were also conducted. Segments with a building density of 0 and over 0.35 (calculated without height information), or 0 and over 4 (calculated with height information) were excluded. The lower limit was set because the aim was to analyze built-up areas. The upper limits were selected on the basis of the scatter plot figures (Figure 5), which suggest that a linear relationship between the mean values and building density only exist when the building density is not very high. The correlation coefficients and coefficients of determination (R^2 values) for different image channels are shown in Table 4.

The scatter plot figures (Figure 5) and the linear regression results (Table 4) show that a clear dependence exists between the building density of an area and its mean intensity and coherence in the image data. For intensity, this result is in accordance with Dong *et al.* (1997), who suggested that a good correlation between the backscattering response and bulk size and density of buildings could be found if the effect of the buildings' orientation is compensated. In the present study, however, such compensation was not made. The highest correlation coefficient (0.811) and coefficient of determination (0.657) were obtained for segment brightness. The correlation values obtained when building heights were taken into account were generally somewhat lower than those obtained without height information. The reasons for this behavior are difficult to determine due to the complex dependencies of the intensity and coherence on various radar system parameters and environmental factors, such as imaging geometry and orientation of buildings (see e.g., Dong *et al.*, 1997; Xia and Henderson, 1997; Fanelli *et al.*, 2001; Luckman and Grey, 2003). The dataset also consisted of a large number of images preprocessed in various steps.

The results suggest that classification of built-up areas into building density classes might be a feasible approach to refine the classification of built-up areas in cases where the area is not very densely built-up (in our dataset the threshold value is about 0.3 to 0.4, calculated as the proportion of land covered with buildings). To determine rules for such a classification, the built-up segments under analysis (Test Site 1) were divided into three classes according to the building densities calculated from the maps (calculated without building heights): (a) sparsely built-up (building density >0, <0.1), (b) intermediately built-up (0.1 to 0.2), and (c) densely built-up (>0.2). Segments for which densities calculated from both the old and new maps belonged to the same class were included. Histograms of segment brightness in the three classes were formed and are shown in Figure 6.

Building Density Classification

Threshold values determined from the histograms of Figure 6 were applied to classify built-up areas of the best land-use classification result (channels 2 through 6 and 8, entire study area) further into three building density classes. As described in the Methods Section, this classification was applied to larger segments than those used in land-use classification. The segmentation and classification results are shown in Plates 2d and 2e.

The accuracy of the building density classification was estimated by comparing the results with building densities calculated from the building maps of Test Site 2 (segments completely covered with the building maps were considered; building densities were calculated without building heights). The results are shown in Table 5. The building densities were calculated separately from the old and new building maps. Only those segments for which both densities belonged to the same class (no buildings (building density 0), very sparse (>0, <0.05), sparse (≥ 0.05, <0.1), intermediate (0.1 to 0.2), or dense (>0.2)) were included in accuracy estimation. The calculated values should therefore accurately represent the situation at the time of image acquisition. Other segments were labeled as undetermined in the table. Sparsely built-up areas determined from the reference data were divided into two classes (very sparse and sparse) to separately account for segments with very low building densities. For example, one building might exist in an otherwise forest-covered segment, and in this case forest could be a better classification than sparsely built-up, although definitive criteria for correct classification cannot be set.

Table 5 shows that the results of building density classification were mainly satisfactory. As the building density calculated from the reference maps increased, the building density estimated from the image data also generally increased. However, since the building density is a continuous variable, the classes cannot be strictly separated from each other in the imagery. For example, when the building density in the maps was sparse (≥ 0.05, <0.1), the percentages of sparsely, intermediately and densely built-up segments in the classification result were 38 percent, 49 percent, and 4 percent, respectively. When the density in the maps was intermediate, the percentages were 12 percent, 62 percent, and 23 percent, and when the density was high, the percentages were 0 percent, 60 percent, and 40 percent. In each

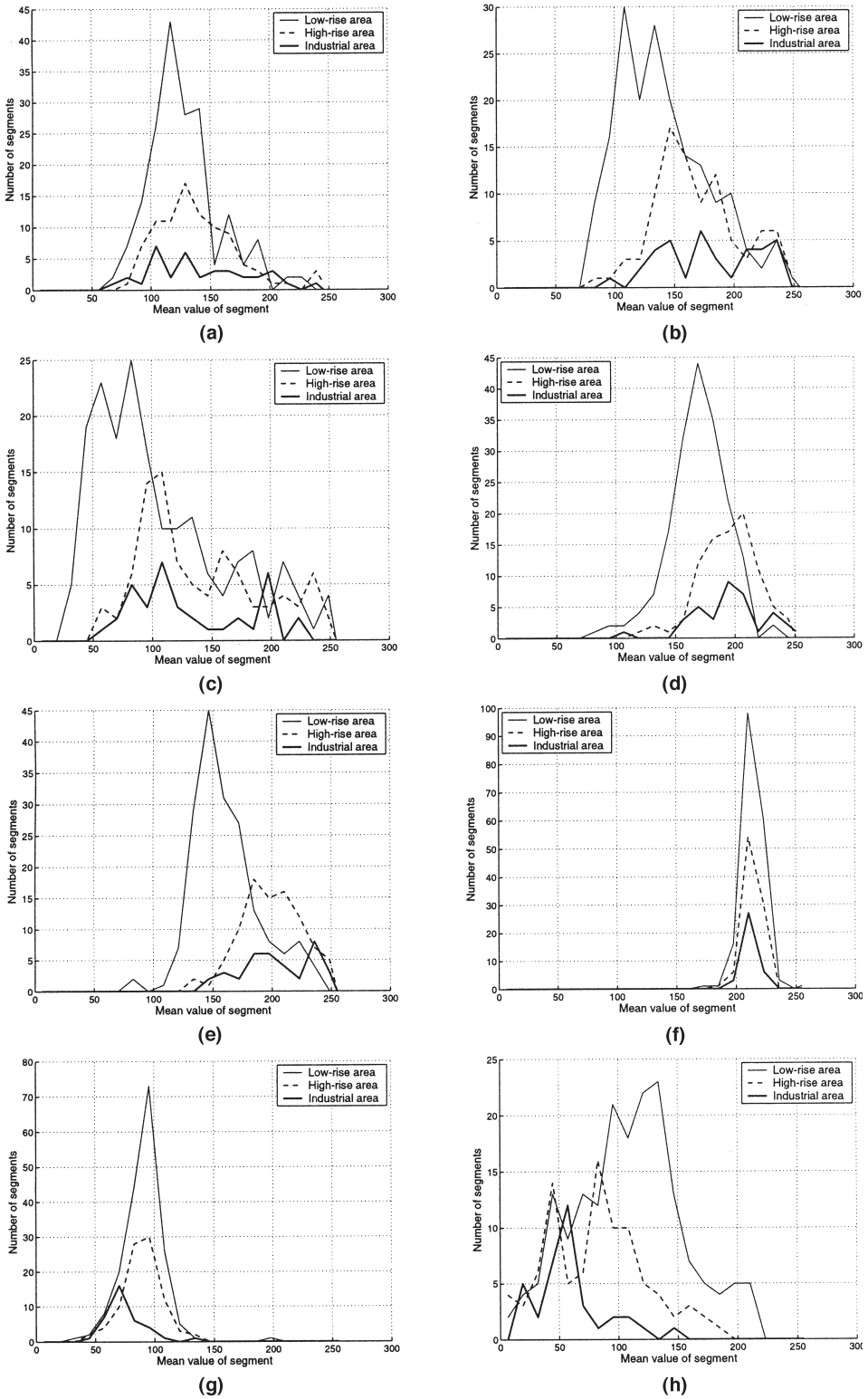

Figure 4. Histograms of the mean values of segments in low-rise areas, high-rise areas and industrial areas. The histograms are shown for each image channel: (a) Intensity, mean, (b) Coherence, mean, (c) Long-time coherence, mean, (d) Coherence, PC1, (e) Coherence, PC2, (f) Intensity, PC1, (g) Intensity, PC2, and (h) Texture.

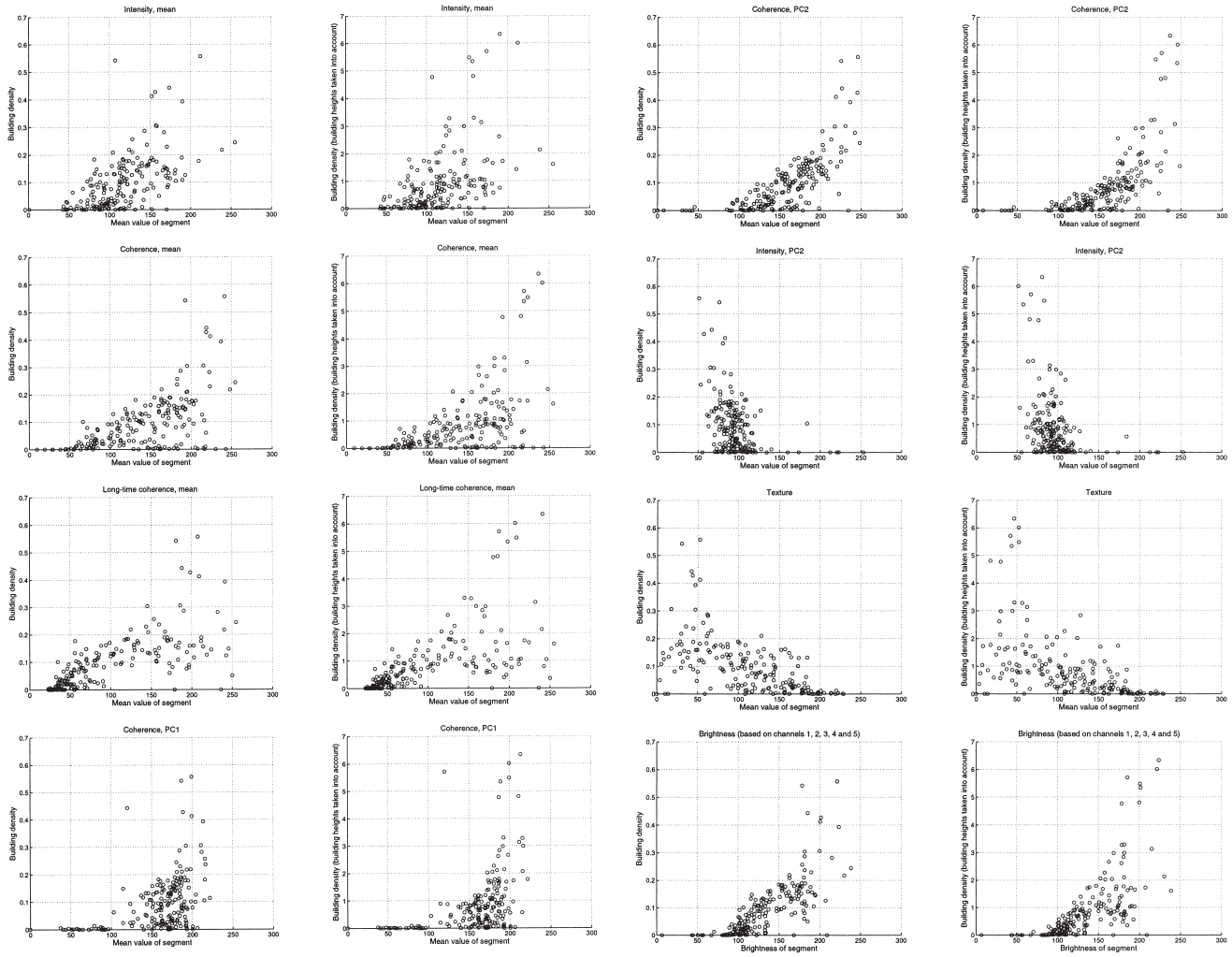

Figure 5. Scatter plots showing the relationship between the mean values or brightness (the last two figures) of segments and building density. The scatter plots are shown for each image channel, except for channel 6, in which the correlation was lowest (see Table 4).

TABLE 4. CORRELATION COEFFICIENTS AND R^2 VALUES FOR THE RELATIONSHIP BETWEEN THE MEAN VALUES OR BRIGHTNESS (LAST ROW) OF SEGMENTS AND BUILDING DENSITY. SEGMENTS WITH A BUILDING DENSITY >0 AND <0.35 (CALCULATED WITHOUT BUILDING HEIGHTS) OR >0 AND <4 (CALCULATED WITH BUILDING HEIGHTS) WERE INCLUDED

Image Channel	Correlation Coefficient		R^2	
		*		*
Intensity, mean	0.590	0.471	0.348	0.222
Coherence, mean	0.584	0.507	0.341	0.257
Long-time coherence, mean	0.740	0.638	0.548	0.408
Coherence, PC1	0.459	0.474	0.210	0.224
Coherence, PC2	0.770	0.732	0.593	0.535
Intensity, PC1	0.248	0.215	0.062	0.046
Intensity, PC2	−0.318	−0.255	0.101	0.065
Texture	−0.667	−0.589	0.445	0.347
Brightness (based on channels 1 through 5)	0.811	0.725	0.657	0.526

*Building heights taken into account.

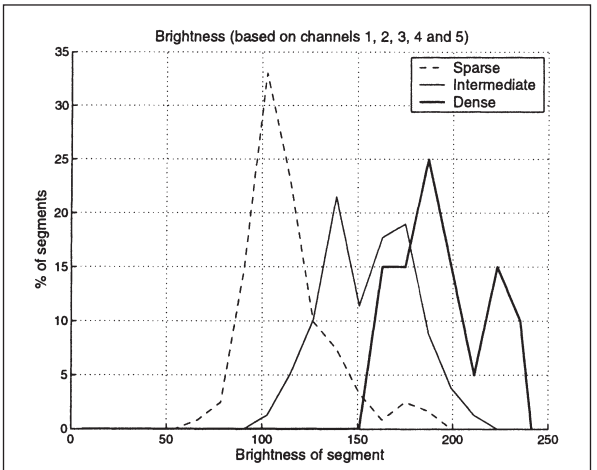

Figure 6. Histograms of segment brightness in three building density classes.

TABLE 5. COMPARISON OF BUILDING DENSITY CLASSIFICATION RESULTS WITH REFERENCE DATA (NUMBER AND PERCENTAGE OF SEGMENTS CLASSIFIED INTO DIFFERENT CLASSES)

	Building Density in Reference Data						
Classification Result	No Buildings (building density 0)	Very Sparse (>0,<0.05)	Sparse (≥0.05,<0.1)	Intermediate (0.1–0.2)	Dense (>0.2)	Undetermined	Sum
Forest	14 (29%)	88 (56%)	4 (9%)	0 (0%)	0 (0%)	10	116
Open area	26 (53%)	29 (18%)	0 (0%)	1 (4%)	0 (0%)	6	62
Built-up, sparse (building density <0.1)	3 (6%)	29 (18%)	18 (38%)	3 (12%)	0 (0%)	19	72
Built-up, intermediate (0.1–0.2)	3 (6%)	11 (7%)	23 (49%)	16 (62%)	3 (60%)	33	89
Built-up, dense (>0.2)	0 (0%)	0 (0%)	2 (4%)	6 (23%)	2 (40%)	8	18
Unclassified	3 (6%)	1 (1%)	0 (0%)	0 (0%)	0 (0%)	0	4
Sum	49	158	47	26	5	76	361

case, the percentage of segments classified into the intermediate class was highest, although the percentage of sparsely built-up segments clearly decreased and that of densely built-up segments increased as the building density in the maps increased. It should be noted, however, that only five segments belonged to the reference class densely built-up, and those results are thus not very reliable.

Further Development

The results of the study suggest that interferometric SAR data are well-suited for distinguishing built-up areas from forest and open areas and for dividing built-up areas into subclasses according to building density. For practical applications, further investigations of the validity of the results and optimization of various parameter values would be useful.

For example, the number of interferometric image pairs used in creating the dataset was large (14), which is one reason for the high quality of the dataset and results. The results presented by Karjalainen *et al.* (unpublished report, 2003) suggest that good land-use classification results could be obtained with a smaller number of images (3 to 6). Grey and Luckman (2003) also achieved high accuracy in urban/non-urban classification from single ERS coherence images with long temporal baselines (the best overall accuracy and kappa coefficient over 90 percent compared with a set of test polygons). Testing the effect of the number of images on the quality of the classification results could be a subject of future research.

Another subject for further research could be optimization of the various parameter values used in segmentation and classification. Default values of the software and values found heuristically were used in the present study. It is possible that even better results could be obtained if the parameters were selected more carefully. On the basis of experiments carried out in the study, we suppose, however, that minor changes in the parameter values would not have a remarkable effect on the results.

Conclusions

A high accuracy was achieved when a multitemporal interferometric ERS dataset was used to distinguish built-up areas from forest and open areas using a region-based classification approach. The overall classification accuracy compared with reference points was 97 percent. Low-rise areas were the most difficult built-up areas to detect. Compared with the reference points, 94 percent of these were detected as built-up. Compared with topographic map data, the percentage was 78 percent. The classification process was highly automatic and resulted in homogeneous regions resembling a map drawn by a human interpreter. As also presented in many previous studies, the results show that interferometric SAR data including coherence information in addition to backscatter intensity is a useful data source for land-use mapping. Additionally, the results confirm that contextual information in the form of texture or neighborhood relationships between segments is advantageous in detecting built-up areas.

The feasibility of the imagery for dividing built-up areas further into subclasses was also investigated. Built-up classes of Finnish 1:50 000 topographic maps (low-rise areas, high-rise areas, and industrial areas) appeared to be difficult to distinguish reliably from each other. On the other hand, a correlation between the building density of an area and its intensity and coherence in the image data was detected in cases where the building density was not very high (threshold value of about 0.3 to 0.4, calculated as the proportion of land covered with buildings). The dataset thus appeared to be promising for classifying built-up areas into subclasses according to building density. Such a classification was tested, and satisfactory results were obtained.

Results of the study suggest that further development of automatic methods for land-use mapping and map updating from interferometric SAR data is possible. It can be expected that such methods will have high potential in the future, especially when interferometric spaceborne SAR images with higher spatial resolution become available.

Acknowledgments

The authors wish to thank Mika Karjalainen and Yannick Devillairs who participated in preprocessing of the building maps. The authors also wish to thank the European Space Agency (ESA, Announcement of Opportunity studies, project number AO3-277) for providing the SAR data and the National Land Survey of Finland and FM-Kartta Oy for providing the map data for the study. The financial support of the National Technology Agency of Finland (TEKES) and the Academy of Finland (project: "Novel map updating with remote sensing imagery", 2003 to 2006) is gratefully acknowledged. The roles of the authors were the following: Marcus Engdahl was responsible for creating the interferometric SAR dataset (interferometric processing, geocoding, and other SAR image preprocessing operations) and collection of the reference points, the study was advised by Juha Hyyppä, and other duties and analyses were carried out by Leena Matikainen.

References

Askne, J., and J.O. Hagberg, 1993. Potential of interferometric SAR for classification of land surfaces, *Proceedings of IGARSS'93: Better Understanding of Earth Environment*, 18–21 August, Tokyo, Japan, IEEE, New York, New York, pp. 985–987.

Baatz, M., and A. Schäpe, 2000. Multiresolution segmentation – An optimization approach for high quality multi-scale image segmentation, *Angewandte Geographische Informationsverarbeitung XII: Beiträge zum AGIT-Symposium Salzburg 2000* (J. Strobl, T. Blaschke, and G. Griesebner, editors), Wichmann, Heidelberg, pp. 12–23.

Bentabet, L., S. Jodouin, D. Ziou, and J. Vaillancourt, 2003. Road vectors update using SAR imagery: A snake-based method, *IEEE Transactions on Geoscience and Remote Sensing*, 41(8): 1785–1803.

Benz, U.C., P. Hofmann, G. Willhauck, I. Lingenfelder, and M. Heynen, 2004. Multi-resolution, object-oriented fuzzy analysis of remote sensing data for GIS-ready information, *ISPRS Journal of Photogrammetry and Remote Sensing*, 58: 239–258.

Blaes, X., and P. Defourny, 2003. Retrieving crop parameters based on tandem ERS 1/2 interferometric coherence images, *Remote Sensing of Environment*, 88:374–385.

Borghys, D., C. Perneel, and M. Acheroy, 2002. Automatic detection of built-up areas in high-resolution polarimetric SAR images, *Pattern Recognition Letters*, 23:1085–1093.

Dammert, P.B.G., J.I.H. Askne, and S. Kühlmann, 1999. Unsupervised segmentation of multitemporal interferometric SAR images, *IEEE Transactions on Geoscience and Remote Sensing*, 37(5): 2259–2271.

Definiens Imaging, 2003. *eCognition, Object Oriented Image Analysis*, User Guide 3, Definiens Imaging GmbH, München, Germany.

Definiens Imaging, 2004. Definiens Imaging GmbH, München, Germany, URL: http://www.definiens.com/, (last date accessed: 15 March 2006).

Dekker, R.J., 2003. Texture analysis and classification of ERS SAR images for map updating of urban areas in The Netherlands, *IEEE Transactions on Geoscience and Remote Sensing*, 41(9):1950–1958.

Del Frate, F., J. Lichtenegger, and D. Solimini, 1999. Monitoring urban areas by using ERS-SAR data and neural networks algorithms, *Proceedings of IGARSS'99: Remote Sensing of the System Earth – A Challenge for the 21st Century*, 28 June – 02 July, Hamburg, Germany, IEEE, Piscataway, New Jersey, pp. 2696–2698.

Dell'Acqua, F., and P. Gamba, 2003. Texture-based characterization of urban environments on satellite SAR images, *IEEE Transactions on Geoscience and Remote Sensing*, 41(1):153–159.

Dierking, W., and H. Skriver, 2002. Change detection for thematic mapping by means of airborne multitemporal polarimetric SAR imagery, *IEEE Transactions on Geoscience and Remote Sensing*, 40(3):618–636.

Dong, Y., B. Forster, and C. Ticehurst, 1997. Radar backscatter analysis for urban environments, *International Journal of Remote Sensing*, 18(6):1351–1364.

Dong, Y., A.K. Milne, and B.C. Forster, 2001. Segmentation and classification of vegetated areas using polarimetric SAR image data, *IEEE Transactions on Geoscience and Remote Sensing*, 39(2):321–329.

Engdahl, M.E., M. Borgeaud, and M. Rast, 2001. The use of ERS-1/2 Tandem interferometric coherence in the estimation of agricultural crop heights, *IEEE Transactions on Geoscience and Remote Sensing*, 39(8):1799–1806.

Engdahl, M.E., and J.M. Hyyppä, 2003. Land-cover classification using multitemporal ERS-1/2 InSAR data, *IEEE Transactions on Geoscience and Remote Sensing*, 41(7):1620–1628.

ER Mapper, 2002. *ER Mapper User Guide*, Earth Resource Mapping, Inc.

Fanelli, A., M. Santoro, A. Vitale, P. Murino, and J. Askne, 2000. Understanding ERS coherence over urban areas, *Proceedings of ERS-Envisat Symposium: Looking Down to Earth in the New Millennium*, 16–20 October, Gothenburg, Sweden, European Space Agency, ESA Publications Division, ESTEC, Noordwijk, The Netherlands, unpaginated CD-ROM.

Fanelli, A., M. Ferri, M. Santoro, and A. Vitale, 2001. Analysis of coherence images over urban areas in the extraction of buildings heights, *Proceedings of IEEE/ISPRS Joint Workshop on Remote Sensing and Data Fusion over Urban Areas*, 08–09 November, Rome, Italy, unpaginated CD-ROM.

Fransson, J.E.S., G. Smith, J. Askne, and H. Olsson, 2001. Stem volume estimation in boreal forests using ERS-1/2 coherence and SPOT XS optical data, *International Journal of Remote Sensing*, 22(14):2777–2791.

GAMMA Remote Sensing, 2004. GAMMA Remote Sensing Research and Consulting AG, Bern, Switzerland, URL: http://www.gamma-rs.ch/, (last date accessed: 15 March 2006).

Gluch, R., 2002. Urban growth detection using texture analysis on merged Landsat TM and SPOT-P data, *Photogrammetric Engineering & Remote Sensing*, 68(12):1283–1288.

Grey, W., and A. Luckman, 2003. Mapping urban extent using satellite radar interferometry, *Photogrammetric Engineering & Remote Sensing*, 69(9):957–961.

Grey, W.M.F., A.J. Luckman, and D. Holland, 2003. Mapping urban change in the UK using satellite radar interferometry, *Remote Sensing of Environment*, 87:16–22.

Haack, B.N., E.K. Solomon, M.A. Bechdol, and N.D. Herold, 2002. Radar and optical data comparison/integration for urban delineation: A case study, *Photogrammetric Engineering & Remote Sensing*, 68(12):1289–1296.

Helldén, U., 1980. *A Test of Landsat-2 Imagery and Digital Data for Thematic Mapping, Illustrated by an Environmental Study in Northern Kenya*, Lunds Universitets Naturgeografiska Institution, Rapporter och Notiser 47, University of Lund, Lund, Sweden, 63 p.

Hellwich, O., M. Günzl, and C. Wiedemann, 2001. Fusion of SAR/INSAR data and optical imagery for landuse classification, *Frequenz*, 55(3–4):129–136.

Hellwich, O., I. Laptev, and H. Mayer, 2002. Extraction of linear objects from interferometric SAR data, *International Journal of Remote Sensing*, 23(3):461–475.

Henderson, F.M., and Z.-G. Xia, 1997. SAR applications in human settlement detection, population estimation and urban land use pattern analysis: A status report, *IEEE Transactions on Geoscience and Remote Sensing*, 35(1):79–85.

Johnsson, K., 1994. Segment-based land-use classification from SPOT satellite data, *Photogrammetric Engineering & Remote Sensing*, 60(1):47–53.

Karathanassi, V., C. Iossifidis, and D. Rokos, 2000. A texture-based classification method for classifying built areas according to their density, *International Journal of Remote Sensing*, 21(9): 1807–1823.

Kettig, R.L., and D.A. Landgrebe, 1976. Classification of multispectral image data by extraction and classification of homogeneous objects, *IEEE Transactions on Geoscience Electronics*, GE-14(1): 19–26.

Kiema, J.B.K., 2002. Texture analysis and data fusion in the extraction of topographic objects from satellite imagery, *International Journal of Remote Sensing*, 23(4):767–776.

Luckman, A., and W. Grey, 2003. Urban building height variance from multibaseline ERS coherence, *IEEE Transactions on Geoscience and Remote Sensing*, 41(9):2022–2025.

Macrì-Pellizzeri, T., P. Gamba, P. Lombardo, and F. Dell'Acqua, 2003. Multitemporal/multiband SAR classification of urban areas using spatial analysis: Statistical versus neural kernel-based approach, *IEEE Transactions on Geoscience and Remote Sensing*, 41(10): 2338–2353.

The MathWorks, 2004. The MathWorks, Inc., Natick, Massachusetts, United States, URL: http://www.mathworks.com/, (last date accessed: 15 March 2006).

Onana, V.-P., E. Trouvé, G. Mauris, J.-P. Rudant, and E. Tonyé, 2003. Linear features extraction in rain forest context from interferometric SAR images by fusion of coherence and amplitude information, *IEEE Transactions on Geoscience and Remote Sensing*, 41(11):2540–2556.

Pulliainen, J., M. Engdahl, and M. Hallikainen, 2003. Feasibility of multi-temporal interferometric SAR data for stand-level

estimation of boreal forest stem volume, *Remote Sensing of Environment*, 85:397–409.

Quartulli, M., and M. Datcu, 2003. Information fusion for scene understanding from interferometric SAR data in urban environments, *IEEE Transactions on Geoscience and Remote Sensing*, 41(9):1976–1985.

Rajesh, K., C.V. Jawahar, S. Sengupta, and S. Sinha, 2001. Performance analysis of textural features for characterization and classification of SAR images, *International Journal of Remote Sensing*, 22(8):1555–1569.

Santoro, M., A. Fanelli, J. Askne, and P. Murino, 1999. Monitoring urban areas by means of coherence levels, *Proceedings of FRINGE '99: Advancing ERS SAR Interferometry from Applications towards Operations*, 10–12 November, Liège, Belgium, European Space Agency, URL: http://earth.esa.int/pub/ESA_DOC/fringe1999/Papers/santoroP.pdf (last date accessed: 15 March 2006).

Santoro, M., A. Fanelli, J. Askne, and P. Murino, 2000. Urban areas classification with SAR and InSAR signatures, *Proceedings of EUSAR 2000, 3rd European Conference on Synthetic Aperture Radar*, 23–25 May, Munich, Germany, VDE-Verlag, Berlin, pp. 647–650.

Schistad Solberg, A.H., and A.K. Jain, 1997. Texture fusion and feature selection applied to SAR imagery, *IEEE Transactions on Geoscience and Remote Sensing*, 35(2):475–479.

Shaban, M.A., and O. Dikshit, 2001. Improvement of classification in urban areas by the use of textural features: The case study of Lucknow city, Uttar Pradesh, *International Journal of Remote Sensing*, 22(4):565–593.

Smith, G., and J. Askne, 2001. Clear-cut detection using ERS interferometry, *International Journal of Remote Sensing*, 22(18): 3651–3664.

Strozzi, T., and U. Wegmüller, 1998. Delimitation of urban areas with SAR interferometry, *Proceedings of IGARSS'98: Sensing and Managing the Environment*, 06–10 July, Seattle, Washington, IEEE, Piscataway, New Jersey, pp. 1632–1634.

Strozzi, T., P.B.G. Dammert, U. Wegmüller, J.-M. Martinez, J.I.H. Askne, A. Beaudoin, and M.T. Hallikainen, 2000. Landuse mapping with ERS SAR interferometry, *IEEE Transactions on Geoscience and Remote Sensing*, 38(2):766–775.

Tupin, F., I. Bloch, and H. Maître, 1999. A first step toward automatic interpretation of SAR images using evidential fusion of several structure detectors, *IEEE Transactions on Geoscience and Remote Sensing*, 37(3):1327–1343.

Ulaby, F.T., F. Kouyate, B. Brisco, and T.H. Lee Williams, 1986. Textural information in SAR images, *IEEE Transactions on Geoscience and Remote Sensing*, GE-24(2):235–245.

Usai, S., and R. Klees, 1999. SAR interferometry on a very long time scale: A study of the interferometric characteristics of man-made features, *IEEE Transactions on Geoscience and Remote Sensing*, 37(4):2118–2123.

Wegmüller, U., and C.L. Werner, 1995. SAR interferometric signatures of forest, *IEEE Transactions on Geoscience and Remote Sensing*, 33(5):1153–1161.

Wegmüller, U., and C. Werner, 1997. Retrieval of vegetation parameters with SAR interferometry, *IEEE Transactions on Geoscience and Remote Sensing*, 35(1):18–24.

Weydahl, D.J., 2001. Analysis of ERS SAR coherence images acquired over vegetated areas and urban features, *International Journal of Remote Sensing*, 22(14):2811–2830.

Xia, Z.-G., and F.M. Henderson, 1997. Understanding the relationships between radar response patterns and the bio- and geophysical parameters of urban areas, *IEEE Transactions on Geoscience and Remote Sensing*, 35(1):93–101.

(Received 13 July 2004; accepted 05 October 2004; revised 28 January 2005)